Structure of the Complex of L-Benzylsuccinate with Wheat Serine Carboxypeptidase II at 2.0-Å Resolution[†,‡]

Timothy L. Bullock,[§] Bruce Branchaud,[∥] and S. James Remington*[,⊥]

Institute of Molecular Biology and Departments of Physics, Chemistry, and Biology, University of Oregon, Eugene, Oregon 97403

Received February 23, 1994; Revised Manuscript Received June 10, 1994[⊗]

ABSTRACT: The structure of the complex of L-benzylsuccinate (K_i = 0.2 mM) bound to wheat serine carboxypeptidase II has been analyzed at 2.0-Å resolution for native and inhibited crystals at −170 °C. The model has been refined and has a standard crystallographic *R*-factor of 0.176 for 57 734 reflections observed between 20.0- and 2.0-Å resolution. The root mean square deviation from ideal bonds is 0.017 Å and from ideal angles is 2.6°. The model consists of 400 amino acids, 4 N-linked saccharide residues, and 430 water molecules. L-Benzylsuccinate occupies a narrow slot in the active site defined by Tyr 60, Tyr 239, and the polypeptide backbone. One carboxylate forms hydrogen bonds to Glu 145, Asn 51, the amide of Gly 52, and the catalytic His 397, suggestive of how the peptide C-terminal carboxylate is recognized by the enzyme. The phenyl ring stacks between Tyr 239 and Tyr 60, while the other carboxylate occupies the "oxyanion hole". One of the oxygens accepts hydrogen bonds from the amides of Tyr 147 and Gly 53, while the other forms a very close contact (2.3 Å) with the Oγ of Ser 146, forcing the side chain into a conformation alternative to that found in the resting state of the enzyme. The inhibitor occupies the active site in a way that suggests that it can be regarded as a transition-state analogue of serine carboxypeptidases. The model suggests a novel enzymatic mechanism, involving substrate-assisted catalysis, that might account for the low pH optimum (4.0–5.5) of peptidase activity unique to this family of serine proteinases.

Carboxypeptidase WII (CPD-WII)[1] from wheat bran (Breddam et al., 1987) is a serine proteinase that specifically removes basic or hydrophobic amino acids from the C-terminus of peptide substrates. The three-dimensional model of the enzyme, refined to 2.2 Å (Liao et al., 1992), revealed a "catalytic triad", Asp 338-His 397-Ser 146, similar to that found in the trypsin and subtilisin families of serine proteinases. However, the overall fold of the polypeptide backbone does not resemble that of any previously solved serine proteinases but rather falls into a recently described class of α/β hydrolase-fold enzymes (Ollis et al., 1992). Substrate-binding motifs common to other serine proteinases (Steitz et al., 1969; Segal et al., 1971), in which the substrate interacts with the enzyme in an extended antiparallel β-sheet fashion, are not present in the active site of CPD-WII.

A major difference between serine carboxypeptidases and the trypsin and subtilisin families of serine proteinases concerns the pH dependence of catalytic activity toward peptide substrates. It is optimum at pH 4.5–5.5 depending on the enzyme, whereas trypsin and subtilisin are optimally active at basic pH. It has been shown for the yeast vacuolar enzyme (CPD-Y) that the falloff of activity at pH >5.5 is due to a drastic increase in K_m, most likely due to dissociation of Glu 145 and consequent unfavorable electrostatic interactions with the carboxylate of the substrate (Mortensen et al., 1994).

Serine carboxypeptidases exhibit two general classes of substrate specificity. CPD-Y preferentially hydrolyzes substrates terminating in hydrophobic amino acids, while CPD-WII can efficiently hydrolyze either bulky hydrophobic or basic substrates with preference for the latter (Breddam et al., 1987). This suggested that the active site of CPD-WII contains at least two binding subsites of dual specificity, S_1 and S_1' [notation of Schechter and Berger (1967)], capable of accepting lysine, arginine, or phenylalanine at the respective positions, P_1 and P_1', in the substrate.

To begin examination of the basis for the substrate specificity of CPD-WII, the structure of the enzyme/product complex containing arginine had previously been determined (Liao et al., 1992). The binding of the amino acid defines a putative S_1' site that accounts for the preferential hydrolysis for positively charged side chains at P_1' (Breddam, 1988). The alkyl portion of the side chain occupied a channel formed by Tyr 239 and Tyr 60, while the positively charged guanidinium group was near two acidic side chains, Glu 398 and Glu 272, and several presumed water molecules. This charge complementarity at the end of the binding site is consistent with the high affinity for substrates terminating in basic residues, and it was suggested that nonpolar side chains would bind in a similar manner (Liao et al., 1992), stacking between Tyr 239 and Tyr 60.

In order to further characterize substrate binding modes, the structure of L-benzylsuccinate (BZS) bound to CPD-WII was investigated. L-Benzylsuccinate resembles a C-terminal phenylalanine residue, with the difference that an OH group replaces the α-carbon of the preceding amino acid and a CH_2 replaces the amide of the peptide bond (Chart 1). BZS was originally developed as a potent competitive inhibitor of the metalloproteinase carboxypeptidase A (CPA; Byers & Wolfen-

[†] This work was supported by National Science Foundation Grant MCB 9118302 (S.J.R.), National Institutes of Health Predoctoral Traineeship 5 R01 GM 42618-02 (T.B.), and a grant to the Institute of Molecular Biology from the Lucille P. Markey Foundation.

[‡] Coordinates have been deposited in the Brookhaven Protein Data Bank under the filenames 1WHT and 1WHS.

* Address correspondence to this author at the Institute of Molecular Biology [telephone (503) 346-5190].

[§] Institute of Molecular Biology and Department of Biology.

[∥] Institute of Molecular Biology and Department of Chemistry.

[⊥] Institute of Molecular Biology and Department of Physics.

[⊗] Abstract published in *Advance ACS Abstracts,* August 15, 1994.

[1] Abbreviations: BZS, benzylsuccinic acid; CPD-WII, wheat serine carboxypeptidase II; F_o, observed structure factor; F_c, calculated structure factor; rms, root mean square.

0006-2960/94/0433-11127$04.50/0

Chart 1: Oxygen Atom Numbering of Benzylsuccinic Acid (**2**) and Comparison to a C-Terminal Phenylalanine **1**

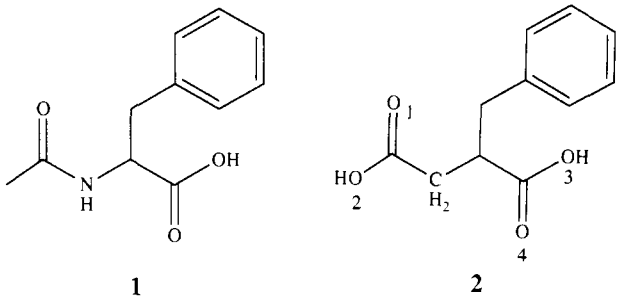

1 **2**

don, 1972). It was termed a "bi-product inhibitor" because of its resemblance to the collected products of peptide hydrolysis. High-resolution crystal structures of BZS bound to carboxypeptidase A (Mangani et al., 1993) and the metalloendopeptidase, thermolysin (Bolognesi & Matthews, 1979), have been determined. These structures confirm interactions that are important to substrate binding and catalysis in both enzymes (Matthews, 1988; Christianson & Lipscomb, 1989).

Here, we describe the results of a crystallographic investigation of L-benzylsuccinate binding to wheat serine carboxypeptidase II at 2.0-Å resolution. The structure permits a rationalization for dual specificity at S_1'. Furthermore, the hydrogen-bonding contacts to the analogue of the C-terminal carboxylate support the suggested roles of Glu 145 and Asn 51 in recognition of the carboxy terminus of peptide substrates (Mortensen et al., 1994).The model also suggests a possible mechanism for proteolysis at low pH, a reaction that serine endoproteinases do not efficiently catalyze. The low activity of the serine endoproteinases at acidic pH has been explained by the requirement for an uncharged histidine to assist in the nucleophilic attack of the serine on the substrate (Blow et al., 1969; Bachkovchin & Roberts, 1978). If one assumes that the enzymatic mechanism of serine carboxypeptidases is similar to that of the endopeptidases, this leads to two possible, but unattractive, hypotheses: either His 397 has a pK_a of $\lesssim 3$, as k_{cat} does not approach 0 at low pH (Mortensen et al., 1994), or the enzyme can work with a protonated histidine. We suggest that the substrate carboxylate participates in the reaction mechanism in a manner that may help to explain the unusually low pH optimum for activity. In this proposal, Glu 145 and Glu 65 form a hydrogen-bond network with the substrate carboxylate that might act as a "proton sink", deprotonating His 397, which then allows the standard serine proteinase mechanism to proceed.

MATERIALS AND METHODS

The inhibition of D,L-benzylsuccinic acid (BZS, Sigma) for CPD-WII-catalyzed hydrolysis of furylacryloyl-Phe-Phe-OH (Sigma) was analyzed at 0, 0.1, 0.2, and 0.4 mM BZS. Reactions were carried out in the presence of 80 nM enzyme active sites, 35 mM sodium chloride, and 5 mM sodium acetate, pH 5.5 at 20 °C. The initial velocity of hydrolysis of the substrate at three concentrations was followed at 337 nm (Remington & Breddam, 1994) with a Shimadzu 2101 scanning spectrophotometer. Kinetic parameters were determined by nonlinear regression using the program NONLIN by Michael Johnson.

Crystals of CPD-WII were grown as described by Wilson et al. (1990). A large ($0.3 \times 0.5 \times 1.0$ mm^3) native crystal was equilibrated against a cryoprotectant solution of 60% (v/v) glycerol, 0.1 M NaCl, 5 mM acetate, pH 5.5, prior to data collection, then mounted in a 1.5×1.0 mm wire loop (Teng, 1990), and quickly placed in a stream of cold, dry nitrogen (−170 °C) for data collection on an Raxis-II imaging plate camera (Molecular Structure Corp.). Graphite monochromated Cu Kα radiation was generated by a Rigaku RU-200 rotating anode operated at 40 kV and 150 mA. Atmospheric absorption was reduced by a helium chamber placed between the crystal and detector. A total of 60° of oscillation data were collected in 54 h using a single sweep with a crystal to detector distance of 280 mm and a 2Θ angle of 15°. There was no apparent decay in the diffraction pattern during data collection.

Diffraction data for a single inhibitor-soaked crystal [equilibrated against 65% (v/v) glycerol, 0.1 M NaCl, 12 mM D,L-BZS, and 5 mM acetate, pH 5.5, for 3 days] were also collected at −170 °C using a detector distance and 2Θ angle of 140 mm and 12°, respectively, in order to obtain higher resolution data.

Crystallographic refinement was performed with the TNT package of programs (Tronrud et al., 1987) and XPLOR (Brünger et al., 1987). Due to unit cell dimension changes, rigid body refinement was required, followed by conventional coordinate refinement using simulated annealing with XPLOR (Brünger et al., 1987) and conjugate direction refinement with TNT (Tronrud, 1992). Manual model rebuilding was performed using the FRODO program (Jones, 1978).

Deviations between the native (4 °C) and frozen (−170 °C) structures were analyzed using a distance-difference plot (Nishikawa et al., 1972). The differences in distance between corresponding α-carbon pairs in the two structures were plotted and contoured on a two-dimensional grid, which reveals local structural perturbations.

Table 1: Data Collection and Atomic Model Statistics for Native and Inhibited Crystals at −170 °C

	native	BZS
resolution (Å)	2.3[a]	2.0
unit cell *a* (Å)	95.6	95.5
unit cell *c* (Å)	208.8	208.6
no. of obsd reflections	52849	185798
no. of unique reflections	29338	57926
completeness (%)	72	87
R_{merge} (%)[b]	4.8	7.7
R-factor[c]	0.175	0.176
atoms	3683	3741
deviations from ideality		
bonds (Å)	0.012	0.017
angles (deg)	2.3	2.6
restrained *B*-factors (Å^2)	4.3	3.8

[a] The detector parameters limited the data collection resolution for the native crystal. [b] $R_{merge} = \sum|I_i - \langle I\rangle|\sum I_i$, where I_i is an individual measurement of average intensity $\langle I\rangle$. [c] The standard crystallographic *R*-factor; $R = \sum|F_o - F_c|/\sum F_o$.

RESULTS

Inhibition by Benzylsuccinic Acid. From the kinetic studies and results of nonlinear regression, K_i of benzylsuccinate for CPD-WII was found to be 0.206 ± 0.02 mM for the racemic mixture. For the substrate, $K_m = 0.67 \pm 0.15$ mM and $k_{cat} = 5200 \pm 800$ min^{-1}. As judged from double-reciprocal plots, the inhibition appears to be strictly competitive.

Low-Temperature Data Collection. CPD-WII crystallizes in space group $P4_12_12$ as described by Wilson et al. (1989). Data collection statistics for native and inhibitor-soaked crystals are provided in Table 1. Compared to data collected at room temperature, both R_{merge} and mean intensity improve at higher angles. This increase in diffraction quality permitted

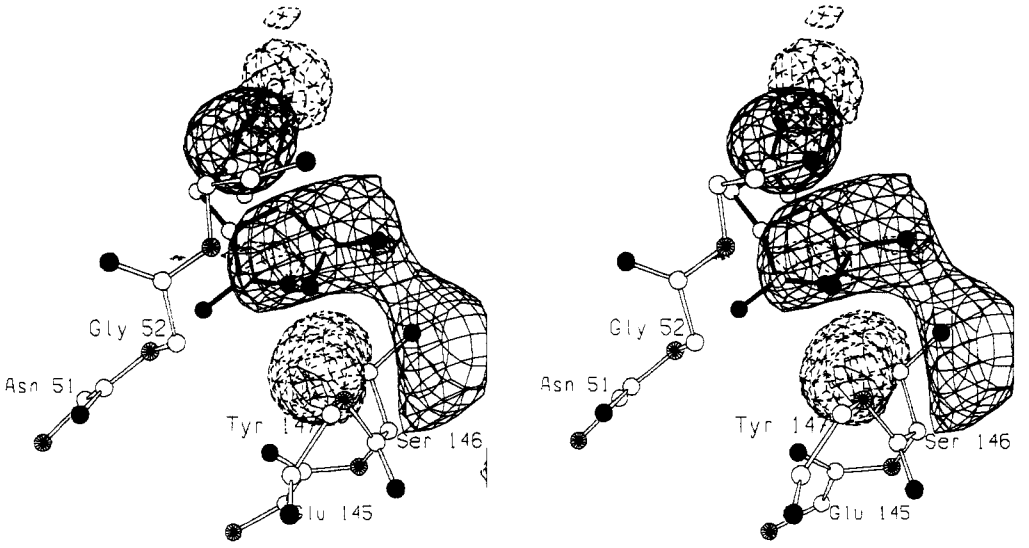

FIGURE 1: 3.3-Å $F_{o,BZS} - F_{o,native}$ difference electron density map using data collected at −170 °C. Phases were taken from the refined model of the native −170 °C structure. The map is contoured at ±4 SD. The positions of the inhibitor and protein backbone of residues 145–146 and 51–53 from the refined CPD-WII/BZS structure are shown. Oxygen atoms are filled; nitrogen atoms are shaded.

data to be collected to a limiting resolution of 2.0 Å at −170 °C as opposed to 2.7 Å at room temperature [2.2 Å at 4 °C using synchrotron radiation (Liao et al., 1992)]. However, concomitant with freezing, the crystals undergo a reduction in unit cell lengths. In general, *a* decreases by about 3 Å and *c* decreases by about 1 Å upon freezing, which led us to collect both native and inhibitor data sets at this temperature.

Changes in the overall protein structure due to freezing included an increase in the number of solvent molecules localized and a small concerted shift of residues 180–240, as judged from a plot of the differences in Cα–Cα distance between the −170 °C structure and the 4 °C structure (not shown). Residues 180–240 constitute a three-helix bundle on the surface of the monomer and participate in forming the dimer interface. Cα–Cα distances do not change appreciably within the bundle or within the rest of the protein. However, Cα–Cα distances between this region and the rest of the protein generally decrease by about 0.5 Å. Movement of the helical bundle and the net negative difference in Cα–Cα distances across the protein indicate an overall compaction of the structure and partially account for the observed decrease in cell constants upon freezing.

Crystallographic Refinement. Due to the changes in cell constants, it was desirable to generate a model for the native protein at −170 °C prior to calculating a difference map for the benzylsuccinate complex. The 4 °C model (Liao et al., 1992), without water or carbohydrate, was refined as a rigid body against 50-Å to 5-Å data, followed with coordinate refinement by simulated annealing which resulted in a model with an *R*-factor of 26.4% for all data to 2.3 Å and reasonable stereochemistry. After several cycles of manual rebuilding and crystallographic refinement, a total of 383 water, 6 saccharide, 1 glycerol, and 2 acetate molecules were located in the structure by inspection of calculated $F_o - F_c$ and $2F_o - F_c$ difference maps. The *R*-factor for the native structure at −170 °C is at 0.175 for 29 384 observed reflections with good geometry (Table 1).

A $F_{(inh,-170°C)} - F_{(nat,-170°C)}$ map was calculated to verify the presence of the inhibitor. On the basis of this map (Figure 1), the side chain of Ser 146 was removed from the starting model because of its proximity to the inhibitor density and the presence of paired positive and negative density, indicating a change of conformation at this residue. The map also revealed a conformational change at Met 238 and Gln 233. These two residues and all water, sugar, acetate, and glycerol molecules were also removed. Upon inspection of a difference electron density map, 275 of the waters were replaced. Refinement of this model against 2.5-Å data from the inhibited crystal led to an $F_o - F_c$ map which showed density for all parts of the inhibitor and for the new conformation of serine 146. This map clearly showed the position and orientation of the benzyl group and two carboxyl groups, making the assignment of stereochemistry unambiguous. Only L-benzylsuccinate is bound to the enzyme. In the course of further refinement, clear density appeared for 4 carbohydrate residues and 155 additional solvent molecules distributed throughout the structure. Water molecules were modeled into difference density peaks greater than 4σ provided at least one hydrogen bond (<3.6 Å) could be made to a polar atom. Figure 2 shows the final $2F_o - F_c$ density for the inhibitor and several surrounding water molecules and side chains and is typical of the overall quality of the map.

The final refined model of BZS/CPD-WII consists of 400 amino acids, 4 N-linked carbohydrate molecules, and 430 water molecules. The crystallographic *R*-factor is 0.176 for all 57 734 reflections observed ($I > 0$) between 20.0- and 2.0-Å resolution, and the geometry is satisfactory (Table 1). Only four non-glycine residues are outside of the "allowed" regions of a Ramachandran diagram. Two of these (308B and 375) are in surface loops with weak density and are probably in error. The other two, Glu 65 at (−130°, −110°) and Ser 146 at (55°, −110°), are in the active site and appear to be constrained to these values by the protein fold (Liao et al., 1992).

Conformational Changes upon Inhibitor Binding. There are large conformational changes of three protein side chains, which caused difference features of about ±10σ in the initial $F_{o,inh} - F_{o,nat}$ difference map. The χ_1 angle of Ser 146 changed by +140° to give a less-strained trans conformation. Fifteen angstroms away from the inhibitor, a coupled rearrangement of Gln 233 and Met 238 also takes place. The movement of these two residues appears to be caused by shifts of Tyr 239 toward Met 238 to accommodate the phenyl group of the inhibitor.

Binding of Benzylsuccinate. L-Benzylsuccinate binds in the same active site location as does the free amino acid arginine

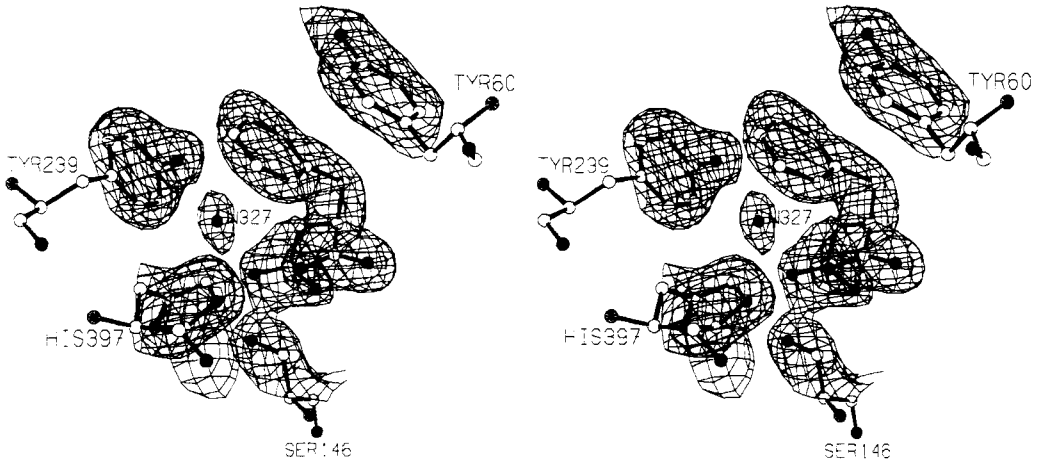

FIGURE 2: Stereo drawing of the final $2F_{o,BZS} - F_c$ density for L-benzylsuccinate and neighboring residues in the active site of CPD-WII for the −170 °C data set using all data from 20.0- to 2.0-Å resolution. The phases were from the final refined model. Contouring is at 1 SD.

(Liao et al., 1992). The benzyl side chain interacts with tyrosines 60 and 239, inserting into a slot about 8 Å wide formed by the parallel rings. The end of this side-chain binding pocket is defined by several acid groups and bound water molecules. An additional nonpolar interaction is made between Cβ of the inhibitor side chain and the Sγ of Cys 56.

The succinic acid portion of the inhibitor (Figure 3a) binds at the bottom of the active site cavity and makes extensive contacts with two peptide strands, including residues 51–53 and 145–147. The inhibitor oxygens participate in a total of seven hydrogen bonds, except that one, O2···Oγ 146, is very short (2.3 Å) and not oriented optimally for hydrogen bonding. The much different pK_as of these two oxygens ($\sim$10 pK_a units) would argue that this close interaction is not an example of a "short strong" hydrogen bond (Cleland, 1992; Gerlt & Gassman, 1993). The hydrogen bonds and their distances are shown in Figure 3a. Comparison to the unliganded active site (Figure 3b) shows that the inhibitor displaces a water molecule (W 252) and a presumed acetate molecule (Ac 460) but does not otherwise disrupt the observed hydrogen-bonding pattern in the active site. Upon inhibitor binding, the hydrogen bond between Glu 145 and Glu 65 lengthens from 2.3 to 2.6 Å. A water molecule (W 327), not seen in the native structure, mediates a hydrogen bond between O2 and tyrosine 239.

Perhaps the most interesting interactions in the inhibited enzyme concern the catalytic histidine (397). In spite of a change of side-chain rotamer, the nucleophilic serine (146) maintains a hydrogen bond with His 397. The histidine reorients slightly such that it makes a perfectly bifurcated hydrogen bond between Oγ of serine 146 and O4 of the inhibitor (Figure 3a). The 2.9-Å N···O bond lengths and the 132° (O4) and 136° (Oγ) NHO bond angles are characteristic of evenly bifurcated hydrogen bonds (Baker & Hubbard, 1984).

In addition to this bifurcated hydrogen bond, the inhibitor O4 oxygen makes an unusual hydrogen bond to the carboxyl group of Glu 145, which in turn is hydrogen bonded to Glu 65 in a similar interaction. This type of interaction also occurs in the CPD-WII/arginine structure (Liao et al., 1992). However, the C4 carboxylate is rotated 67° with respect to the carboxylate of arginine and interacts with Glu 145 on the opposite side (anti) of Oε1. O3 maintains the same position seen for a carboxylate oxygen in the arginine complex and accepts hydrogen bonds from the amide of Gly 52 and Nδ1 of Asn 51.

The C1 carboxylate binds directly adjacent to serine 146 with one oxygen (O1) directed toward the peptide nitrogens 53 and 147. The nitrogens are oriented to provide the optimal distance (2.8 Å) and linearity for hydrogen bonding to O1. O2 makes a hydrogen bond with a water molecule (W 327) and a very close contact of 2.3 Å with Oγ of 146, but the geometry is rather poor for hydrogen bonding.

The amide nitrogens of residues 53 and 147 have been suggested to form the "oxyanion hole" of CPD-WII by structural comparison to trypsin and subtilisin (Liao et al., 1992). The C1 carboxylate of L-benzylsuccinate is in a good position to take advantage of the oxyanion stabilization proposed for this region [for a review, see Ménard and Storer (1992)]. To make this interaction, the inhibitor binds more deeply in the active site than does arginine (Figure 4). This closer association may force the altered terminal (C4) carboxylate binding observed for L-benzylsuccinate as opposed to that observed for arginine.

DISCUSSION

The enzymatic activities of CPD-WII and other serine carboxypeptidases are well characterized (Breddam, 1987; Breddam et al., 1988). They display a variety of substrate specificities in both the S_1 and S_1' substrate-binding sites. CPD-WII shows a dual specificity that is characteristic of several members of this class and has maximal peptidase activity at low pH, a feature common to all serine carboxypeptidases. In order to investigate these characteristics of the activity, we have determined the structure of the enzyme complexed to the putative "bi-product" inhibitor L-benzylsuccinate at −170 °C.

Basis for Dual Specificity at P_1'. The benzyl group of BZS binds in a nonpolar slot formed by tyrosines 60 and 239 (Figure 2). This result accounts for kinetic data showing that CPD-WII tightly binds substrates with a P_1' phenylalanine. The gap, which is large enough to accommodate all other nonpolar side chains, also accounts for the ability of CPD-WII to efficiently hydrolyze alanine, valine, isoleucine, and methionine (Breddam et al., 1987).

The structural basis for dual specificity is apparent from the overlay of bound benzylsuccinate and arginine (Figure 4). The side chains superimpose, indicating that S_1' does not consist of two subsites but, rather, of one site that accepts either type of amino acid, basic and hydrophobic. Because the naturally occurring basic amino acids, lysine and arginine, possess long alkyl side chains, they are stabilized by the hydrophobic cleft while the basic termini extend into a hydrophilic, negatively charged region beyond the cleft as described previously (Liao

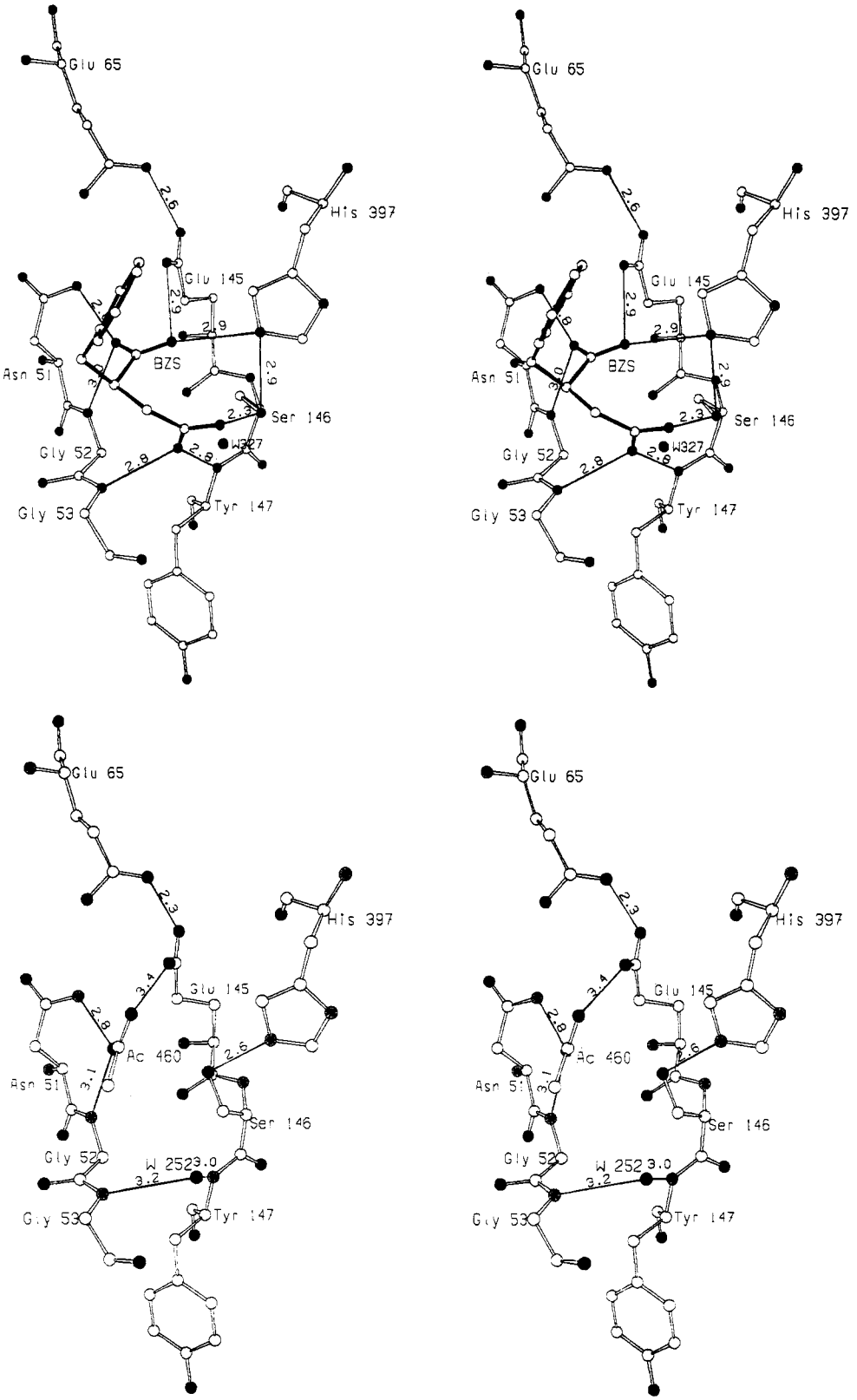

FIGURE 3: (a, top) Stereo pair of the refined L-benzylsuccinate molecule viewed from the exterior of the active site. The seven hydrogen bonds to the protein are shown as thin lines and have the indicated lengths in angstroms. (b, bottom) Active site of the refined native model at −170 °C shown from the same perspective as in (a). A putative acetate and water molecule provide several of the same interactions made by BZS in the CPD-WII/BZS complex. In particular, the acetate molecule appears to mimic the binding of a substrate carboxylate.

et al., 1992). Shorter, hydrophobic side chains would be stabilized by the two parallel aromatic rings but would not extend into the polar end of the cleft.

Binding of Inhibitor Carboxylates. The region of the enzyme that is responsible for recognition of the C-terminal carboxylate of a substrate had been tentatively identified on the basis of the binding of arginine (Liao et al., 1992) and confirmed by mutagenesis (Mortensen et al., 1994). In the CPD-WII/L-benzylsuccinate structure, the C4 carboxylate occupies this area. It makes hydrogen bonds with the side-chain nitrogen of Asn 51, the backbone amide of Gly 52, the carboxylate of Glu 145, and Nε1 of His 397. While Asn 51,

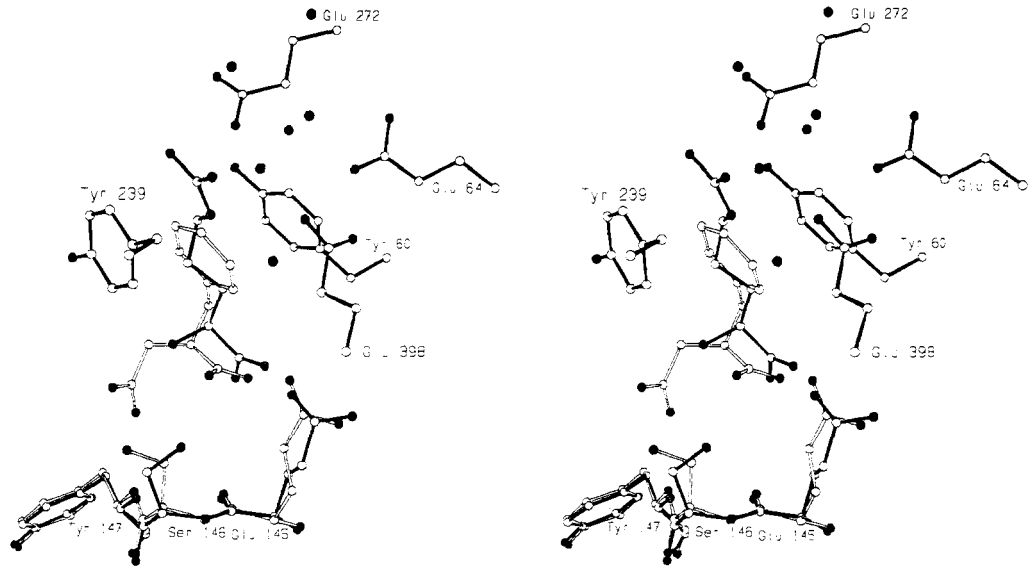

FIGURE 4: Stereoview of bound arginine (solid bonds) and L-benzylsuccinate (open bonds) overlaid in the active site. Residues 145–147 from both models are shown. Other surrounding residues are from the model containing arginine (filled bonds). The structures were overlaid on the basis of a least-squares superposition of all Cα atoms of the two enzyme models. The filled spheres are water molecules observed in the structure containing arginine.

Gly 52, and His 397 donate hydrogen bonds, the role of Glu 145 as donor or acceptor is unclear in the absence of information on its protonation state in the complex. It has been shown that the enzyme recognizes the charged form of the substrate carboxylate by virtue of protonated Glu 145 (Mortensen et al., 1994). However, it is clear that deprotonation of both carboxylates would lead to charge exclusion at the terminal binding site and an increased K_m for peptides at high pH. This provides a reasonable explanation for the strong pH dependence of K_m observed in serine carboxypeptidases (Breddam, 1985; Mortensen et al., 1994).

The C1 carboxylate of L-benzylsuccinate binds in a restricted region formed by Ser 146 and the amides of residues 147 and 53. By analogy to the well-studied serine endoproteinases, the amides are expected to stabilize the negatively charged tetrahedral intermediate of peptide hydrolysis (Robertus et al., 1972). L-Benzylsuccinate simulates this oxyanion interaction well, as judged from the excellent hydrogen-bonding geometry at this site.

Is Benzylsuccinate a "Bi-Product" Inhibitor? L-Benzylsuccinate has been designated a bi-product inhibitor of zinc carboxypeptidase A (CPA) on the basis of the resemblance to the "collected products" of peptide hydrolysis (Byers & Wolfendon, 1973). The high affinity of the inhibitor for CPA is attributed to additive effects of binding at both the peptide and amino acid product sites. The structure of the inhibitor bound to CPA (Mangani et al., 1992) supports this proposal. The benzyl ring and C4 carboxylate occupy the S_1' site of the enzyme and terminal carboxylate binding site while the C1 carboxylate coordinates the active site zinc in a bidentate manner similar to an enzyme/product complex (Christianson & Lipscomb, 1987). The C4 carboxylate binds as expected for the carboxylate of a peptide substrate (Christianson & Lipscomb, 1989), making a salt bridge with arginine 145 and hydrogen bonds to tyrosine 248 and asparagine 144. An unusual hydrogen bond, similar to the one between the glutamate 145 of CPD-WII and BZS, also occurs in the CPA complex. In this case, glutamate 270, the presumed general base in the proteolytic reaction, makes a hydrogen bond to the C1 carboxylate, and thus a carboxylate oxygen may occupy the site normally occupied by the nucleophilic water molecule. Glu 270 was assumed to be protonated, since the inhibitor has been shown to bind as the dianion (Palmer et al., 1982).

Benzylsuccinic acid has higher affinity for carboxypeptidase A than for CPD-WII. K_i is 1×10^{-6} M for the racemic mixture toward CPA (Byers & Wolfendon, 1973) but only 0.21 mM toward CPD-WII, a 200-fold increase. Part of this tighter binding can be attributed to charge–charge interactions with CPA. The active site zinc and arginine 145 both interact with the inhibitor. On CPD-WII, there is a smaller degree of electrostatic stabilization. The inhibitor makes only one interaction with a potential countercharge, histidine 397.

In CPA, hydrolysis occurs via the enzyme-promoted attack of a water molecule on the bound substrate, resulting in simultaneous formation of peptide and amino acid products (Christianson & Lipscomb, 1989). For serine carboxypeptidases, the relevance of the proposed bi-product inhibition is not clear because of the two-step nature of the reaction. The peptide and amino acid products are formed at different times and do not occupy the active site simultaneously. There are fewer constraints on the distance between binding sites since some rearrangements could occur between the release of the amino acid product and hydrolysis of the acyl-enzyme intermediate. Therefore, benzylsuccinate cannot be considered a bi-product inhibitor of serine carboxypeptidases. The observed dissimilarity in carboxylate binding between a true product, arginine, and L-benzylsuccinate supports this hypothesis.

Benzylsuccinate as a Transition-State Analogue? Although BZS is not a particularly good inhibitor of serine carboxypeptidases, there are reasons for consideration of its mode of binding as at least partially resembling the first transition state for peptide hydrolysis, the formation of the first tetrahedral intermediate. The CPD-WII/L-BZS structure shows some characteristics proposed for the formation of the covalent tetrahedral intermediate. As pointed out, BZS closely resembles a C-terminal phenylalanyl residue, a good substrate for the enzyme. The nucleophilic serine 146 is in the productive "trans" conformation seen in covalent peptide inhibitors of trypsin and chymotrypsin (Richardson, 1970; Rühlman et al., 1973; Blow et al., 1974), and the Oγ is in contact (2.8 Å) with the inhibitor at C1, resembling the proposed geometry of the nucleophilic attack. An oxygen atom accepts two hydrogen bonds from peptide nitrogens 147

Scheme 1: Proposal for the Reaction Mechanism of Serine Carboxypeptidases at Low pH[a]

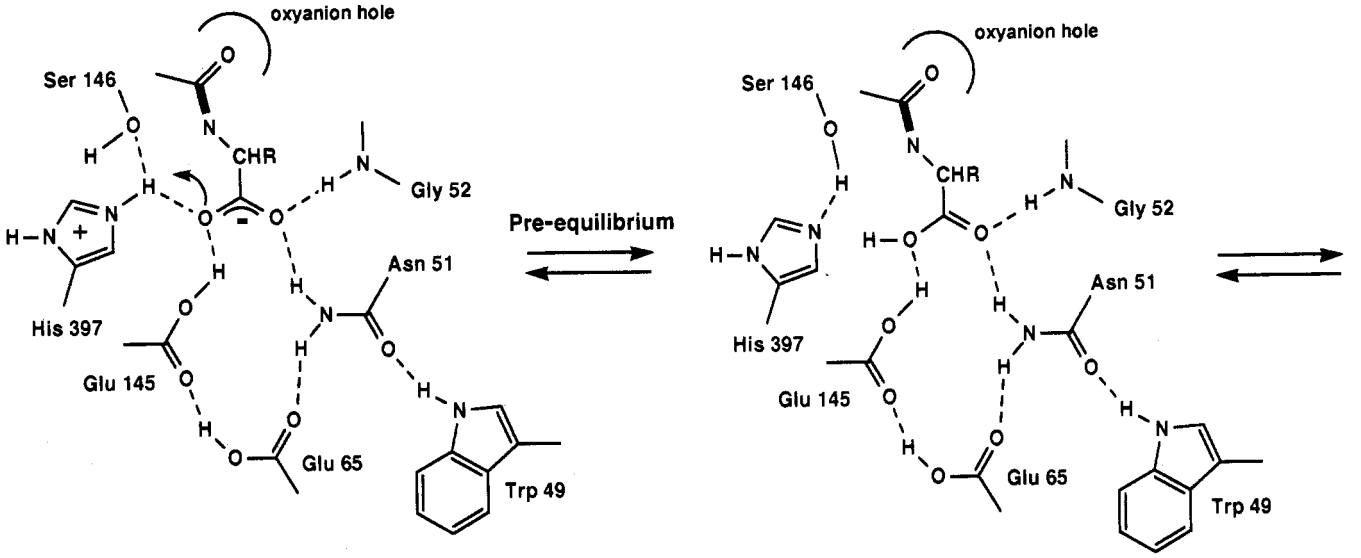

[a] It is assumed that the catalytic His 397 has a normal pK_a and is normally protonated in the Michaelis complex at the pH of maximum activity (pH 4.0–5.5). A proton transfer from the catalytic His 397 to the carboxylate of a peptide substrate generates a neutral histidine, and the normal serine proteinase mechanism follows. The scissile peptide bond is drawn with a thick line, and R is the P_1' side chain of the substrate.

and 53 analogous to the oxyanion interaction revealed in inhibited serine proteinases (Delbaere & Brayer, 1985; Bone et al., 1987). Finally, C2 has tetrahedral geometry as is expected for nitrogen in the equivalent position of the tetrahedral intermediate just prior to cleavage of the scissile bond.

The relatively poor binding of BZS to CPD-WII may be rationalized as due to bad contacts between Ser 146 Oγ and C1 (2.8 Å) and O2 (2.3 Å). These would not occur with BZS bound to carboxypeptidase A since the nucleophilic water of CPA can be displaced by the inhibitor. For these reasons, we suggest that BZS can be considered to be a transition-state analogue for serine carboxypeptidases. It may be possible to design much more potent inhibitors of these enzymes by taking the mode of binding into consideration.

Mechanistic Implications of the CPD-WII/BZS Structure. The bifurcated arrangement of serine 146, histidine 397, and the terminal carboxylate of BZS was not seen in the CPD-WII/arginine product complex and has implications for reaction intermediate formation in serine carboxypeptidases. As with serine endoproteinases the histidine and serine are essential for full activity (Blow, 1976; Carter & Wells, 1988; Bech & Breddam, 1989). Given the existence of a catalytic triad Asp-His-Ser in all three families of serine proteinases, it is reasonable to assume that the most important features of the mechanism of serine endopeptidases are also utilized by serine carboxypeptidases, that is, that proton transfer from the catalytic serine to the histidine is required either before or during nucleophilic attack of the serine on the substrate (Bachovchin & Roberts, 1978).

However, unlike trypsin and subtilisin, k_{cat} for serine carboxypeptidases does not approach 0 at low pH and only changes by a factor of 4.5 in the pH range 3.0–6.5 (Mortensen et al., 1994). This has led to the suggestion that the essential histidine has a pK_a of <3. If indeed it is this low, two serious problems are presented. First, transfer of a proton from Ser 146 to His 397 would be energetically inconsistent with the observed rate of catalysis [~200 s^{-1} for a good substrate (Breddam, 1985)]. From the Arrhenius equation

$$k = A \exp(-\Delta G^{\ddagger}/RT)$$

the energy barrier ($\Delta G^{\ddagger}$) for the rate-limiting step of the reaction can be estimated. Making the standard assumption that the unimolecular preexponential factor A is 10^{13} s^{-1} for a pseudo-unimolecular reaction proceeding from the Michaelis complex, the energy barrier relative to the ground state is about 14.5 kcal/mol. However, proton transfer from a serine with pK_a ~ 15.7 to a histidine with pK_a ~ 2.5 costs at least 18.5 kcal/mol ($-RT$ ln ΔK_a), assuming that there is no significant barrier to proton transfer between O and N beyond the energetic difference between the two protonation states. Second, given the overall structural similarity of the catalytic triads of trypsin and CPD-WII, there are no obvious features in the active site of CPD-WII that would satisfactorily account for a perturbation of the histidine pK_a from its solution value of 6.5 to <3.

An alternative possibility is that the histidine has a normal pK_a and would thus be protonated at the pH for optimal activity (4.0–5.5). If the histidine must accept a proton from the serine, the enzyme must have some means to deprotonate the histidine prior to this transfer. In the CPD-WII/BZS complex, the C4 carboxylate, which is involved in a network of hydrogen bonds that includes Glu 145 and Glu 65, also makes a hydrogen bond with His 397. This suggests that the substrate carboxylate, or the network to which it is hydrogen bonded, might act as a proton sink for His 397. Scheme 1 illustrates one of the many possible mechanisms for this initial step of the reaction, in which an acid–base preequilibrium is postulated. Transfer of a proton from the protonated histidine to the substrate carboxylate neutralizes both, and then the normal mechanism of the serine proteinase catalyzed hydrolysis can proceed. Although such a transfer will probably be somewhat endothermic, it should be rapid and provide reasonable transient amounts of the deprotonated, neutral histidine for normal catalysis to proceed even at very acidic pH values.

There is some kinetic evidence in favor of this hypothesis. The enzyme binds peptide substrates only in the charged form at low pH (Mortensen et al., 1994). The pH dependence of hydrolysis for C-terminal amino acid amides and esters, which cannot participate in the proposed proton transfer, is very different than with peptides. They are hydrolyzed optimally at basic pH, and catalysis falls off at low pH, consistent with

the titration of a group of pK_a ~ 6, which may be His 397 (Breddam, 1985). Mutational replacement of Glu 145 with Gln or Ala causes a 100-fold reduction in k_{cat} but does not alter K_m for peptide substrates, suggesting that the interaction of Glu 145 with the substrate carboxylate, in the previously described hydrogen-bond network, plays an important role in the transition state (Mortensen et al., 1994). Finally, the charged substrate carboxylate in the proximity of the active site serine would disfavor formation of the negatively charged serine alkoxide or tetrahedral intermediate (Bachovchin & Roberts, 1978), and our proposal appears to remove this objection. Certainly more information about pK_as of active site groups, and those of substrate analogues when bound to the enzyme, will be required before these ideas can be more fully developed.

NOTE ADDED IN PROOF

After submission of this paper, our attention was drawn to the work of Christensen (1994), who has proposed the same acid–base preequilibrium on the basis of kinetic studies with several substrates for yeast serine carboxypeptidase. This author showed that the pH dependence of the reaction can be completely accounted for by a detailed kinetic model that takes this proposed proton transfer to substrate, or possibly Glu 145, into account.

ACKNOWLEDGMENT

We thank Dr. Klaus Breddam for generous gifts of purified CPD-WII and Dr. Uffe Mortensen for helpful discussions.

REFERENCES

Bachovchin, W. W., & Roberts, J. D. (1978) *J. Am. Chem. Soc. 100*, 8041–8047.
Baker, E. N., & Hubbard, R. E. (1984) *Prog. Biophys. Mol. Biol. 44*, 97–179.
Blow, D. M. (1976) *Acc. Chem. Res. 9*, 145–152.
Blow, D. M., Birktoft, J. J., & Hartley, B. S. (1969) *Nature 221*, 337–348.
Blow, D. M., Janin, J., & Sweet, R. M. (1974) *Nature 249*, 54–57.
Bolognesi, M. C., & Matthews, B. W. (1979) *J. Biol. Chem. 254*, 634–639.
Bone, R., Shenvi, A. B., Kettner, C. A., & Agard, D. A. (1987) *Biochemistry 26*, 7609–7614.
Breddam, K. (1985) *Carlsberg Res. Commun. 50*, 309–323.
Breddam, K. (1986) *Carlsberg Res. Commun. 51*, 83–128.
Breddam, K., Sørensen, S. B., & Svendsen, I. (1987) *Carlsberg Res. Commun. 52*, 297–311.
Brünger, A. T., Kuriyan, J., & Karplus, M. (1987) *Science 235*, 458–460.
Byers, L. D., & Wolfendon, R. (1972) *J. Biol. Chem. 247*, 606–608.
Byers, L. D., & Wolfendon, R. (1973) *Biochemistry 12*, 2070–2078.
Carter, P., & Wells, J. A. (1988) *Nature 332*, 564–568.
Christensen, U. (1994) *Eur. J. Biochem. 220*, 149–153.
Christianson, D. W., & Lipscomb, W. N. (1987) *J. Am. Chem. Soc. 109*, 5536–5538.
Christianson, D. W., & Lipscomb, W. N. (1989) *Acc. Chem. Res. 22*, 62–69.
Cleland, W. W. (1992) *Biochemistry 31*, 317–319.
Delbaere, L. T. J., & Brayer, G. D. (1985) *J. Mol. Biol. 183*, 89–103.
Gerlt, J. A., & Gassman, P. G. (1993) *J. Am. Chem. Soc. 115*, 11552–11568.
Henderson, R. (1970) *J. Mol. Biol. 54*, 341–354.
Jones, A. T. (1978) *Acta Crystallogr. A43*, 489–501.
Liao, D. I., Breddam, K., Sweet, R. M., Bullock, T., & Remington, S. J. (1992) *Biochemistry 31*, 9796–9812.
Mangani, S., Carloni, P., & Orioli, P. (1992) *J. Mol. Biol. 223*, 573–578.
Matthews, B. W. (1988) *Acc. Chem. Res. 21*, 333–340.
Ménard, R., & Storer, A. C. (1992) *Biol. Chem. Hoppe-Seyler 373*, 393–400.
Mortensen, U., Remington, S. J., & Breddam, K. (1994) *Biochemistry 33*, 508–517.
Nishikawa, K., Ooi, T., Isogai, Y., & Saitô, N. (1972) *J. Phys. Soc. Jpn. 32*, 1331–1337.
Ollis, D. L., Cheah, E., Cygler, M., Dykstra, B., Frolow, F., Fraken, S. M., Harel, M., Remington, S. J., Silman, I., Schrag, J., Sussman, J., & Goldman, A. (1992) *Protein Eng. 5*. 197–211.
Palmer, A. R., Ellis, P. D., & Wolfenden, R. (1982) *Biochemistry 21*, 5056–5059.
Remington, S. J., & Breddam, K. (1994) *Methods Enzymol.* (in press).
Robertus, J. D., Kraut, J., Alden, R. A., & Birktoft, J. J. (1972) *Biochemistry 11*, 4293–4303.
Rühlman, A., Kukla, D., Schwager, P., Bartels, K., & Huber, R. (1973) *J. Mol. Biol. 77*, 417–436.
Schechter, I., & Berger, A. (1967) *Biochem. Biophys. Res. Commun. 27*, 157–162.
Segal, D. M., Powers, J. C., Cohen, G. H., Davies, D. R., & Wilcox, P. E. (1971) *Biochemistry 10*, 3728–3737.
Steitz, T. A., Henderson, R., & Blow, D. M. (1969) *J. Mol. Biol. 46*, 337.
Teng, T. Y. (1990) *J. Appl. Crystallogr. 23*, 387–391.
Tranchemontagne, J., Michaud, L., & Potier, M. (1990) *Biochem. Biophys. Res. Commun. 168*, 22–29.
Tronrud, D. E. (1992) *Acta Crystallogr. A48*, 912–916.
Tronrud, D. E., Ten Eyck, L. F., & Matthews, B. W. (1987) *Acta Crystallogr. A43*, 489–501.
Wilson, K. P., Liao, D. I., Bullock, T. L., Remington, S. J., & Breddam, K. (1990) *J. Mol. Biol. 211*, 301–303.
Zhou, X. Y., Galjart, N. J., Willemson, R., Gillemans, N., Galjaard, H., & d'Azzo, A. (1991) *EMBO J. 10*, 4041–4048.